Covariant-Projection Quadrilateral Elements for the Analysis of Waveguides with Sharp Edges

Ruth Miniowitz and J. P. Webb, *Member, IEEE*

Abstract—**Covariant-projection elements are shown to be a good way of finding the dispersion characteristics of arbitrarily shaped waveguides. They have been demonstrated to produce no spurious modes, and because only tangential continuity is imposed between elements, either the electric field or the magnetic field may be solved for, in the presence of both dielectric and magnetic materials. Further, waveguides with sharp metal edges may be analyzed more efficiently than with earlier methods. Results are presented for a rectangular waveguide half loaded with dielectric, a double-ridged waveguide, a shielded microstrip line, and coupled microstrip lines on a cylindrical substrate.**

I. Introduction

FINDING the modes of arbitrarily shaped waveguides continues to be a challenging computational problem. Despite the fact that it is two-dimensional, there is still no completely general solution. That is not to say that there has been no progress. Early on, scalar finite difference and finite element methods were developed that are extremely good at finding the TE and TM modes of hollow, convex, metal-walled tubes [1]. However, when different dielectrics are present, the solution involves at least two, coupled field components; i.e., it is vector, rather than scalar. The earliest methods for the vector problem produced spurious modes [2], [3]. Since then, a number of techniques have been proposed to overcome the problem of spurious modes, but each has its drawback, e.g. loss of matrix sparsity [4], [5], a larger number of field components [6], or the need to estimate, either manually [7] or automatically [8], a suitable penalty parameter.

Nevertheless, with these new methods spurious modes are not the obstacle they once were. There remain, however, a number of difficulties in waveguide analysis. One of them, which this paper addresses, is the treatment of singularities. Many waveguides have nonconvex boundaries; that is, they contain sharp metal edges at which the electromagnetic fields are singular. In the scalar case, it seems to be sufficient to refine the mesh around such points, although more sophisticated approaches have been used [9], [10]. The vector case is more difficult. Vector methods capable of avoiding spurious modes have all involved transverse field components, which become infinite at sharp edges. With traditional, Lagrangian finite elements, refining near the edge does not work. One answer is to add singular trial functions [11]. This paper describes an alternative: the use of a different type of finite element.

Manuscript received June 18, 1990; revised October 24, 1990. This work was supported by the Natural Sciences and Engineering Research Council of Canada.

R. Miniowitz was with the Department of Electrical Engineering, McGill University, Montreal, Canada, on leave from the Electromagnetics Department, RAFAEL, P.O. Box 2250, Haifa 31021, Israel. She has since rejoined RAFAEL.

J. P. Webb is with the Department of Electrical Engineering, McGill University, 3480 University St., Montreal, H3A 2A7, Canada.

IEEE Log Number 9041950.

II. The Boundary Value Problem

The time-harmonic magnetic field $\boldsymbol{H}$ in a waveguide satisfies the following vector wave equation:

$$\nabla \times \epsilon_r^{-1} \nabla \times \boldsymbol{H} - k_0^2 \mu_r \boldsymbol{H} = 0 \tag{1}$$

where k_0 is the wavenumber and ϵ_r and μ_r are the relative permittivity and permeability, respectively. The modes of the waveguide are the eigensolutions $(\boldsymbol{H}, k_0)$ of (1) when $\boldsymbol{H}$ is constrained to vary as $\exp(-j\beta z)$, z being the coordinate along the waveguide axis and β the phase constant.

When k_0 is not zero, any solution of (1) also satisfies the divergence equation

$$\nabla \cdot \mu_r \boldsymbol{H} = 0 \tag{2}$$

so it is not necessary to impose this equation separately. However, (1) has an infinite number of static solutions: fields for which k_0 is zero and which are consequently irrotational. A few of the static solutions may be genuine, depending on the waveguide, but most of them do not satisfy the divergence equation and are therefore nonphysical.

In the numerical solution of (1), it is usually the case that some of the computed modes will be exactly irrotational, i.e., exactly static. Because their eigenvalues are zero, they can readily be detected and thrown away. However, in addition, some computed modes may be *inaccurate* approximations to static solutions. Because they are inaccurate, they do not have zero eigenvalues. These are the spurious modes.

To avoid spurious modes, one approach is to reimpose the divergence equation [7], [4]. Another approach is to use a finite element for which *all* approximations to static modes are exact. Simple, rectangular elements of this kind were described by Hano [12], who later generalized them to triangles [13]. Recently, curvilinear quadrilateral elements with the same property were invented [14], and applied to waveguides at cutoff ($\beta = 0$). These are called covariant-projection elements.

III. Covariant-Projection Elements

A covariant-projection element is shown in Fig. 1. Its geometry is the same as that of the curvilinear, isoparametric version of the rectangular, nine-node, Lagrange element [17,

0018-9480/91/0300-0501$01.00 ©1991 IEEE

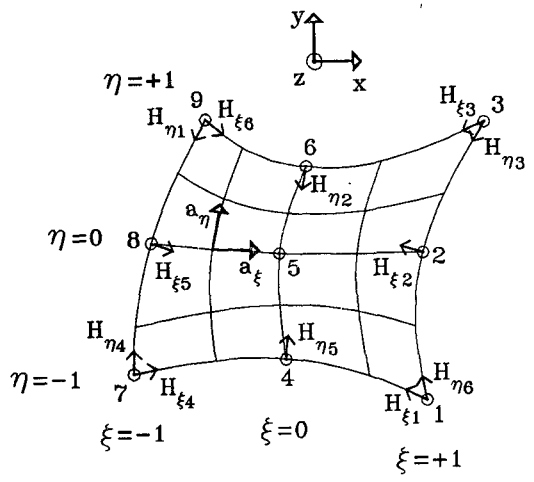

Fig. 1. A covariant-projection element.

p. 119 and sections 8.1 and 8.2]. Each element has a local coordinate system ξ, η that is not necessarily orthogonal but nevertheless can be used to define unitary vectors [15] $\boldsymbol{a}_\xi, \boldsymbol{a}_\eta$ at each point. Following the nomenclature of tensor calculus, the projections of a vector field $\boldsymbol{H}$ on the unitary vectors are called its *covariant* components. They are

$$H_\xi = \boldsymbol{H} \cdot \boldsymbol{a}_\xi \quad \text{and} \quad H_\eta = \boldsymbol{H} \cdot \boldsymbol{a}_\eta. \tag{3}$$

At the edges of the element, these are proportional to the tangential components of $\boldsymbol{H}$. For example, if H_ξ is zero on the edge $\eta = 1$, $\boldsymbol{H}$ is perpendicular to the edge. By using H_ξ and H_η as the unknowns instead of H_x and H_y, it is easy to impose vector boundary conditions and tangential continuity from one element to the next, even at curved boundaries.

After calculating the covariant components one can get the full vector $\boldsymbol{H}$ easily by using the reciprocal vectors, $\boldsymbol{a}^\xi$ and $\boldsymbol{a}^\eta$, defined as follows [15]:

$$\boldsymbol{a}^\xi = \frac{1}{V}(\boldsymbol{a}_\eta \times \boldsymbol{a}_z) \quad \text{and} \quad \boldsymbol{a}^\eta = \frac{1}{V}(\boldsymbol{a}_z \times \boldsymbol{a}_\xi) \tag{4}$$

where V is $\boldsymbol{a}_\xi \cdot (\boldsymbol{a}_\eta \times \boldsymbol{a}_z)$ and $\boldsymbol{a}_z$ is a unit vector in the z direction. In terms of these vectors, the three-component $\boldsymbol{H}$ is

$$H = H_\xi \boldsymbol{a}^\xi + H_\eta \boldsymbol{a}^\eta + jH_z \boldsymbol{a}_z. \tag{5}$$

The factor of j is to account for the 90° phase difference between transverse and axial components for lossless, isotropic waveguides.

The three covariant components of $\nabla \times \boldsymbol{H}$ are

$$j\frac{\partial H_z}{\partial \eta} - \frac{\partial H_\eta}{\partial z} \qquad \frac{\partial H_\xi}{\partial z} - j\frac{\partial H_z}{\partial \xi} \qquad \frac{\partial H_\eta}{\partial \xi} - \frac{\partial H_\xi}{\partial \eta}. \tag{6}$$

Assuming a variation with z of $\exp(-j\beta z)$, these become

$$j\frac{\partial H_z}{\partial \eta} + j\beta H_\eta \qquad -j\beta H_\xi - j\frac{\partial H_z}{\partial \xi} \qquad \frac{\partial H_\eta}{\partial \xi} - \frac{\partial H_\xi}{\partial \eta}. \tag{7}$$

The trial functions for H_ξ and H_η are mixed-order; that is, each trial function for H_ξ is a polynomial of order 2 in η, but order 1 in ξ, and each trial function for H_η is of order 2 in ξ, but order 1 in η (see the Appendix). H_z is second-order in each variable. Because of this mixing of orders, for each component of $\nabla \times \boldsymbol{H}$ both terms are polynomials of the same orders in ξ and η. It has been stated—though a rigorous proof is lacking—that such mixing of orders is sufficient to prevent any inaccurate approximation of irrotational fields, i.e., to eliminate spurious modes [14], [16]. Certainly no spurious modes were detected in any of the problems described below. It is interesting to note that although the earlier rectangular elements of Hano [12] are also mixed-order, the subsequent triangular elements [13] are not.

From (1), each exactly modeled irrotational field corresponds to a frequency of zero and hence gives rise to one zero eigenvalue of the algebraic problem. It is of some interest to know how many such fields there are. Consider a trial $\boldsymbol{H}$ over a mesh of elements, tangentially continuous and satisfying magnetic-wall conditions where necessary. It can be shown that such an $\boldsymbol{H}$ is irrotational if and only if it is the gradient of a scalar function V, with these properties: (a) V can be exactly constructed on the same mesh by taking each quadrilateral as a nine-node Lagrange element and assigning nodal values appropriately; and (b) V is zero on the magnetic walls. The number of irrotational fields is the number of linearly independent scalar functions of this kind, i.e., the total number of nodes in the mesh of nine-node quadrilaterals, minus the number of nodes on the magnetic walls. This equals the number of free H_z values, a result that is also true for Hano's elements [12], [13]. (The above argument holds for $\beta > 0$. When β is zero, some of the irrotational fields might be physical, e.g. the fundamental mode of microstrip at cutoff. It is possible to show, however, that the number of *nonphysical* irrotational fields equals the number of free H_z values in all cases.)

Covariant-projection elements have the additional advantage that they are able to handle sharp edges. Consider two smooth, perfectly conducting surfaces meeting at a sharp edge. The magnetic field must be tangential to each surface all the way up to the edge; i.e., the direction of the field must change discontinously at the edge. This discontinuity cannot be modeled by traditional, C^0 elements, in which all components of the field are continous. With covariant-projection elements, however, only the tangential part of the magnetic field is continuous from element to element; the normal part is allowed to be discontinous. It turns out that this discontinuity is sufficient to allow accurate computation of eigenvalues, even without singular trial functions. The polynomial basis functions do not become infinite at the edge as they should, so the field close to the edge will necessarily be inaccurate. However, the eigenvalues depend on the field over the whole domain, in an integral sense, and they seem relatively insensitive to local errors at the edge, provided the correct discontinuity is allowed for. Of course, refining the mesh near the edge improves the accuracy, and it may well be that singular trial functions could still be used with advantage, but there is none of the pathological behavior associated with C^0 elements.

IV. Computer Program

A FORTRAN computer program has been written using the covariant-projection elements described above. The program solves (1) by the standard variational method and

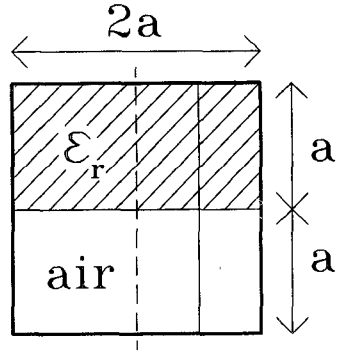

Fig. 2. Cross-section of a rectangular waveguide half loaded with dielectric. The broken line shows the plane of symmetry. $\epsilon_r = 1.5$.

functional (for example, see [12, eq. (11)]). Boundary conditions on the tangential part of the field, as well as tangential continuity between elements, were imposed. As usual, the variational principle reduces to a generalized eigenvalue problem of the form

$$([S] - k_0^2[T])\{H\} = 0 \tag{8}$$

where $[S]$ and $[T]$ are $N \times N$ global matrices after all boundary and continuity conditions are imposed, and $\{H\}$ is an N vector whose components are free values of H_ξ, H_η, and H_z. The matrices $[S]$ and $[T]$ depend on β, which is an input to the program. The integration required to calculate $[S]$ and $[T]$ was carried out numerically using the nine-point Gauss quadrature method [17, p. 174].

The formulation for the electric field is very similar to that given above for the magnetic field, and the program can solve for either. Since only tangential continuity is enforced, there is no difficulty caused by the discontinuity of the normal component of the electric field at dielectric interfaces.

Although the matrices $[S]$ and $[T]$ are sparse, the solutions given below were all obtained with an off-the-shelf, dense-matrix alogrithm—reduction to tridiagonal form followed by bisection. The program ran on a MicroVax II under Ultrix. A problem with $N = 400$ took about one hour of CPU time.

V. Results

Fig. 2 shows a rectangular waveguide half loaded with dielectric. We analyzed half of the structure, with the plane of symmetry taken as a perfect magnetic conductor. The problem was solved with the $\boldsymbol{H}$ formulation. In addition to the mixed-order element described above, a full-order element was tried, i.e., a quadrilateral, curvilinear element in which all three covariant components are interpolated with quadratic trial functions in both ξ and η. Table I shows a comparison of results for the first three true modes. The exact results were computed from transcendental equations found in [18]. The full-order element gave good results for the three modes but also introduced a large number of spurious modes. It is clear that, for the quadrilateral element to work, mixed-order interpolation is necessary.

Consider next the double-ridged waveguide shown in Fig. 3. One quarter of the structure, with boundary conditions for the odd modes, was analyzed at cutoff ($\beta = 0$). We tried both $\boldsymbol{E}$ and $\boldsymbol{H}$ formulations and several refinements of the simple three-element mesh shown in Fig. 3. Table II demonstrates

TABLE I
Comparison of Wavenumbers for the Partially Loaded Waveguide of Fig. 2 for $\beta a = 5.0$ (Asterisk Denotes Spurious Mode)

Mode Number	$k_0 a$ Exact	Mixed Order $\boldsymbol{H}$ $N = 56$	Full Order $\boldsymbol{H}$ $N = 74$
			*4.212
			*4.212
			*4.279
1	4.405	4.406	4.406
2	4.693	4.708	4.708
			*4.991
			*4.991
3	5.136	5.211	5.211

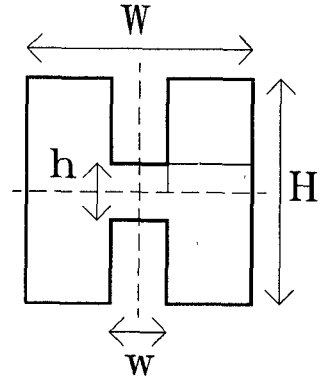

Fig. 3. Cross section of a double-ridged waveguide. The broken lines show the planes of symmetry. $W = 12.7$ mm, $H = 10.16$ mm, $w = 2.54$ mm, and $h = 2.794$ mm.

how well the frequencies of the first three modes converge as the number of elements is increased. These modes are TE, and can be compared with the result of a scalar analysis using fifth-degree, C^1-continuous finite elements [10]. Table II also shows results obtained with two non-finite-element methods.

In addition, the double-ridged waveguide was analyzed at several nonzero values of β. Interestingly, the results agreed exactly with the formula

$$k_0^2 = \beta^2 + k_c^2 \tag{9}$$

when k_c was taken as the value of k_0 given by the program at $\beta = 0$. In other words, for homogeneous waveguides, the method seems to get the form of the dispersion curve exactly right.

The shielded microstrip line is an important problem which has sharp edges, and is one for which a scalar analysis is inadequate. We analyzed one half of the line shown inset in Fig. 4, with a magnetic wall on the plane of symmetry. Again, both $\boldsymbol{E}$ and $\boldsymbol{H}$ formulations were tried, and the initial mesh was refined to check convergence. Fig. 4 gives dispersion curves for the first three modes, using the $\boldsymbol{H}$ formulation and the finest mesh (32 elements). The solid line for the first two modes is obtained from a vector finite-element analysis using singular trial functions [11]. The broken lines represent non-finite-element results: the first mode is from [19]; and the other two are from [20]. Fig. 4 shows good agreement between the various methods. Table III demonstrates the convergence of the dominant mode with increasing mesh refinement for two values of β. If we accept that

TABLE II
CONVERGENCE OF THE CUTOFF WAVENUMBERS k_c (rad/mm) WITH INCREASING NUMBERS OF ELEMENTS FOR THE DOUBLE-RIDGED WAVEGUIDE SHOWN IN FIG. 3

		N	Mode 1	Mode 2	Mode 3
3 elements	H	48	0.1462	0.6427	0.7312
	E	24	0.1402	0.6221	0.6748
12 elements	H	172	0.1444	0.6319	0.7014
	E	120	0.1432	0.6214	0.6735
48 elements	H	624	0.1440	0.6200	0.6723
	E	528	0.1437	0.6197	0.6721
TE scalar C^1 [10]			0.1440	0.6192	0.6713
Montgomery [22]			0.1437	0.6190	0.6712
Utsumi [23]			0.1438	0.6215	0.6707

TABLE III
CONVERGENCE OF k_0 (rad/mm) WITH INCREASING NUMBERS OF ELEMENTS FOR THE DOMINANT MODE OF THE MICROSTRIP SHOWN IN FIG. 4

		N	$\beta = 0.5$ rad/mm	$\beta = 2$ rad/mm
4 elements	H	59	0.1862	0.6958
	E	38	0.3854	0.7699
8 elements	H	119	0.1847	0.6926
	E	71	0.2029	0.7135
16 elements	H	215	0.1937	0.7090
	E	167	0.1941	0.7083
32 elements	H	431	0.1934	0.7083
	E	335	0.1953	0.7110
Webb [11]	H	450	0.2005	0.7209

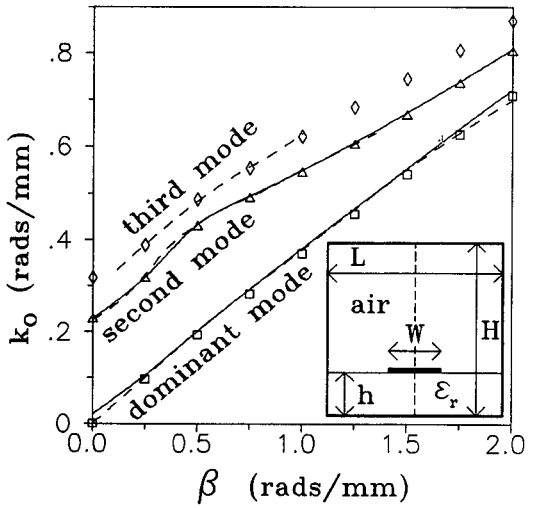

Fig. 4. Dispersion curves for the first three modes of a shielded microstrip transmission line. The broken line in the inset figure shows the plane of symmetry. $L = 12.7$ mm, $W = 1.27$ mm, $h = 1.27$ mm, $H = 12.7$ mm, and $\epsilon_r = 8.875$.

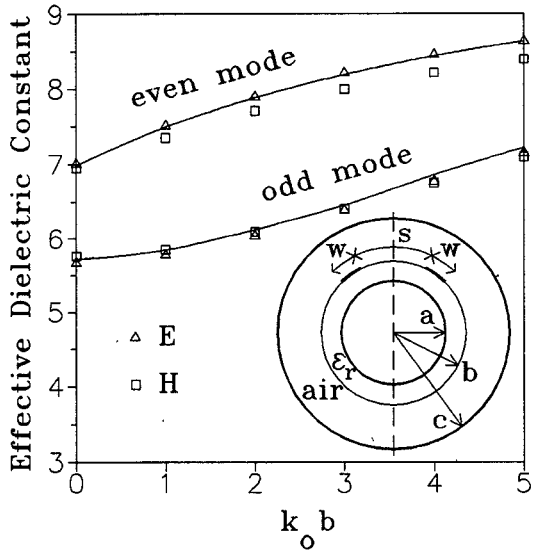

Fig. 5. Dispersion curves for the odd and even modes of coupled microstrip lines on a cylindrical substrate. The broken line in the inset figure shows the plane of symmetry. $a/b = 0.9$, $c/h = 10$, $s/h = 1$, $w/h = 1$, where $h = b - a$. $\epsilon_r = 9.6$. Since the effective dielectric constant is undefined at $k_0 = 0$, the squares and triangles at $k_0 b = 0$ actually have a very small, nonzero frequency, $0 < k_0 b \ll 1$.

the 32-element results are nearest to the true values, then the table shows that covariant-projection elements with about 200 degrees of freedom can give better accuracy than the singular-trial-function method [11] with 450 degrees of freedom.

The last example (Fig. 5) is of coupled microstrip lines on a cylindrical substrate [21]. The problem solved in [21] is unbounded, but to solve it with the present method we introduced an electric wall around the problem, at a distance from the strips that was ten times the substrate thickness. Half of the structure was analyzed, with the plane of symmetry taken as either an electric wall or a magnetic wall, depending on whether the odd or the even mode was required. Fifty elements were used. Their curvilinear nature made it easy to get a good modeling of the circular boundaries and interfaces. Fig. 5 shows the effective dielectric constant, $(\beta/k_0)^2$, obtained with E and H formulations and a comparison with results in [21] (solid line).

VI. CONCLUSIONS

Covariant-projection elements are effective in calculating dispersion curves for arbitrarily shaped waveguides. No spurious modes have been detected. As shown by the microstrip example, the method is able to analyze geometries with sharp edges with fewer degrees of freedom than an earlier technique using singular trial functions.

The matrices generated are sparse, and the number of zero eigenvalues produced is predictable. It therefore seems likely that the algebraic problem can be solved by sparse techniques, which would make the method applicable to even more complicated geometries at a modest computational cost.

APPENDIX

In each element, the magnetic field is interpolated as follows:

$$\boldsymbol{H} = \sum_{i=1}^{6} H_{\xi i} X_i(\xi,\eta)\boldsymbol{a}^{\xi} + \sum_{i=1}^{6} H_{\eta i} Y_i(\xi,\eta)\boldsymbol{a}^{\eta} + j\sum_{i=1}^{9} H_{zi} Z_i(\xi,\eta)\boldsymbol{a}_z$$

where X_i, Y_i, and Z_i are the following trial functions:

$$X_1 = -l_2(\xi)q_1(\eta) \qquad X_4 = l_1(\xi)q_1(\eta)$$
$$X_2 = -l_2(\eta)q_2(\eta) \qquad X_5 = l_1(\xi)q_2(\eta)$$
$$X_3 = -l_2(\xi)q_3(\eta) \qquad X_6 = l_1(\xi)q_3(\eta)$$
$$Y_1 = -q_1(\xi)l_2(\eta) \qquad Y_4 = q_1(\xi)l_1(\eta)$$
$$Y_2 = -q_2(\xi)l_2(\eta) \qquad Y_5 = q_2(\xi)l_1(\eta)$$
$$Y_3 = -q_3(\xi)l_2(\eta) \qquad Y_6 = q_3(\xi)l_1(\eta)$$

$$Z_1 = q_3(\xi)q_1(\eta) \quad Z_4 = q_2(\xi)q_1(\eta) \quad Z_7 = q_1(\xi)q_1(\eta)$$
$$Z_2 = q_3(\xi)q_2(\eta) \quad Z_5 = q_2(\xi)q_2(\eta) \quad Z_8 = q_1(\xi)q_2(\eta)$$
$$Z_3 = q_3(\xi)q_3(\eta) \quad Z_6 = q_2(\xi)q_3(\eta) \quad Z_9 = q_1(\xi)q_3(\eta).$$

The quantities l_1, l_2, q_1, q_2, and q_3 are Lagrange polynomials of degree 1 and 2:

$$l_1(s) = \frac{1}{2}(1-s) \qquad l_2(s) = \frac{1}{2}(1+s)$$

$$q_1(s) = \frac{1}{2}s(s-1) \qquad q_2(s) = (1-s^2) \qquad q_3(s) = \frac{1}{2}s(s+1).$$

Acknowledgment

The authors express their gratitude to C. Crowley for inspiring them to pursue further the application of covariant-projection elements.

References

[1] P. Silvester, "A general high-order finite-element waveguide analysis program," *IEEE Trans. Microwave Theory Tech.*, vol. MTT-21, pp. 538–542, 1969.
[2] P. Daly, "Hybrid-mode analysis of microstrip by finite-element methods," *IEEE Trans. Microwave Theory Tech.*, vol. MTT-19, pp. 19-25, Jan. 1971.
[3] A. Konrad, "Vector variational formulation of electromagnetic fields in anisotropic media," *IEEE Trans. Microwave Theory Tech.*, vol. MTT-24, No. 9, pp. 553–559, 1976.
[4] K. Hayata, M. Koshiba, M. Eguchi, and M. Suzuki, "Vectorial finite-element method without any spurious solutions for dielectric waveguiding problems using transverse magnetic-field component," *IEEE Trans. Microwave Theory Tech.*, vol. MTT-34, pp. 1120–1124, Nov. 1986.
[5] A. J. Kobelansky and J. P. Webb, "Eliminating spurious modes in finite-element waveguide problems by using divergence-free fields," *Electron. Lett.*, vol. 22, no. 11, pp. 569–570, May 22, 1986.
[6] J. A. M. Svedin, "A numerically efficient finite-element formulation for the general waveguide problem without spurious modes," *IEEE Trans. Microwave Theory Tech.*, vol. 37, pp. 1708–1715, Nov. 1989.
[7] B. M. A. Rahman and J. B. Davies, "Penalty function improvement of waveguide solution by finite elements," *IEEE Trans. Microwave Theory Tech.*, vol. MTT-32, pp. 922–928, Aug. 1984.
[8] J. P. Webb, "Efficient generation of divergence-free fields for the finite element analysis of 3D cavity resonances," *IEEE Trans. Magn.*, vol. pp. 162–165, Jan. 1988.
[9] Z. Pantic and R. Mittra, "Quasi-TEM analysis of microwave transmission lines by the finite-element method," *IEEE Trans. Microwave Theory Tech*, vol. MTT-34, pp. 1096–1103, Nov. 1986.
[10] M. Israel and R. Miniowitz, "An efficient finite element method for nonconvex waveguide based on Hermitian polynomials," *IEEE Trans. Microwave Theory Tech.*, vol. MTT-35, pp. 1019–1026, Nov. 1987.
[11] J. P. Webb, "Finite element analysis of dispersion in waveguides with sharp metal edges," *IEEE Trans. Microwave Theory Tech.*, vol. 36, pp. 1819–1824, Dec. 1988.
[12] M. Hano, "Finite-element analysis of dielectric-loaded waveguides," *IEEE Trans. Microwave Theory Tech.*, vol. MTT-32, no. 10, pp. 1275–1279, 1984.
[13] M. Hano, "Vector finite-element solution of anisotropic waveguides using novel triangular elements," *Electron. and Commun. Japan*, part 2, vol. 71, no. 8, pp. 71–80, 1988.
[14] C. W. Crowley, P. P. Silvester, and H. Hurwitz, "Covariant projection elements for 3D vector field problems," *IEEE Trans. Magn.* vol. 24, pp.397–400, Jan. 1988.
[15] J. A. Stratton, *Electromagnetic Theory*. New York: McGraw-Hill, 1941.
[16] C. W. Crowley, "Mixed order covariant projection finite elements for vector fields," Ph.D. thesis, McGill University, 1988.
[17] O. C. Zienkiewicz and J. Taylor, *The Finite-Element Method*, vol. 1, 4th ed. London: McGraw-Hill, 1989.
[18] L. Lewin, *Theory of Waveguides*. New York: Halstead Press, 1975.
[19] R. Mittra and T. Itoh, "A new technique for the analysis of the dispersion characteristics of microstrip lines," *IEEE Trans. Microwave Theory Tech.*, vol. MTT-19, pp. 47–56 Jan. 1971.
[20] D. Mirshekar-Syahkal and J. Brian Davies, "Accurate solution of microstrip and coplanar structures for dispersion and for dielectric and conductor losses," *IEEE Trans. Microwave Theory Tech.*, vol. MTT-27, pp. 694–699, July 1979.
[21] A. Nakatani and N. G. Alexopoulos, "Coupled microstrip lines on a cylindrical substrate," *IEEE Trans Microwave Theory Tech.*, MTT-35, pp. 1392–1398, Dec. 1987.
[22] J. P. Montgomery, "On the complete eigenvalue solution of ridged waveguide," *IEEE Trans. Microwave Theory Tech.*, vol. MTT-19, pp. 547–555, June 1971.
[23] Y. Utsumi, "Variational analysis of ridged waveguide modes," *IEEE Trans. Microwave Theory Tech.*, vol. MTT-33, pp. 111–120, Feb. 1985.

Ruth Miniowitz received the B.Sc., M.Sc., and D.Sc. degrees in mathematics from the Israel Institute of Technology, Haifa, Israel, in 1972, 1975, and 1978 respectively.

Between 1978 and 1983 she was a Visiting Assistant Professor with the mathematics departments of the universities of Maryland, Michigan, Kentucky, and Northern Illinios. Since 1983 she has been a Senior Researcher at RAFAEL Haifa, Israel. During the academic year 1989/90 she was on sabbatical as a visiting scientist at the Computational Analysis and Design Laboratory in the Department of Electrical Engineering, McGill University, Montreal, Canada.

Dr. Miniowitz is a member of the American Mathematical Society and the Israel Union of Mathematics.

J. P. Webb (M'83) received the Ph.D. degree from Cambridge University, England, in 1981.

Since 1982 he has been an Assistant Professor, then an Associate professor, in the Electrical Engineering Department at McGill University, Montreal, Canada. His area of research is computer methods in electromagnetics, especially the application of the finite element method.